

Microstrip-to-Microstrip Interconnects with Adhesive Bonded Ribbons for Micro- and Millimeterwave Applications

Wolfgang Pohlmann, Arne F. Jacob, *Member, IEEE*, and Helmut Schäfer

Abstract—A simple chip-to-chip interconnect technique with adhesive bonded ribbons is presented. It solves the insertion loss problem of wire bond interconnects in micro- and millimeterwave assemblies. The following paper discusses design and fabrication of such interconnects. A quasistatic model is developed to ease the quality assessment of their electrical behavior. It is validated by measurements on microstrip resonators with and without interconnects. The chip-to-chip interconnect technique with adhesive bonded ribbons exhibit low loss and is useable up to 50 GHz or more.

Index Terms—Adhesive bonded joint, chip-to-chip interconnect, dividing-the-capacitance approach, MMIC, M³IC, quasistatic approach, ribbon bond.

I. INTRODUCTION

IN the last few years, much effort was devoted world-wide to the development of microwave monolithic integrated circuits (MMIC's) and millimeterwave monolithic integrated circuits (M³IC's) [1]. With these circuits the cost for micro- and millimeterwave devices can reach a level that makes them attractive for high volume applications like automotive radars, communication units, environmental and industrial sensors. A key element affecting RF performance in microwave modules is the chip-to-chip interconnect. In the recent past many different conceptions of chip interconnects were developed. Examples of these new electrical connection techniques are wire-mesh bonding [2], flip-chip mounting [3], [4], field- and radiation-coupling [5], [6], and adaptive wire- and ribbon-bonding [7]–[10].

The use of bonded ribbons for microstrip-to-microstrip interconnects obviates the parasitic inductance of bond wires. Because of the boundary conditions set by an automatic ribbon bond process with ultrasonic or thermocompression bonding techniques a certain loop height is unavoidable and the width of the ribbon must be smaller than the strip conductor of the microstrip line on the substrate. This small ribbon width and the loop cause increased insertion loss and excess inductance. In contrast to this adhesive bonded ribbons can be made as wide as the same of the microstrip line to be connected, and

Manuscript received December 8, 1997; revised August 25, 1998.

W. Pohlmann and H. Schäfer are with the Fraunhofer-Institute for Applied Materials Research, Bremen 28719, Germany.

A. F. Jacob is with the Institut für Hochfrequenztechnik, Braunschweig 38023, Germany.

Publisher Item Identifier S 1070-9894(98)08526-0.

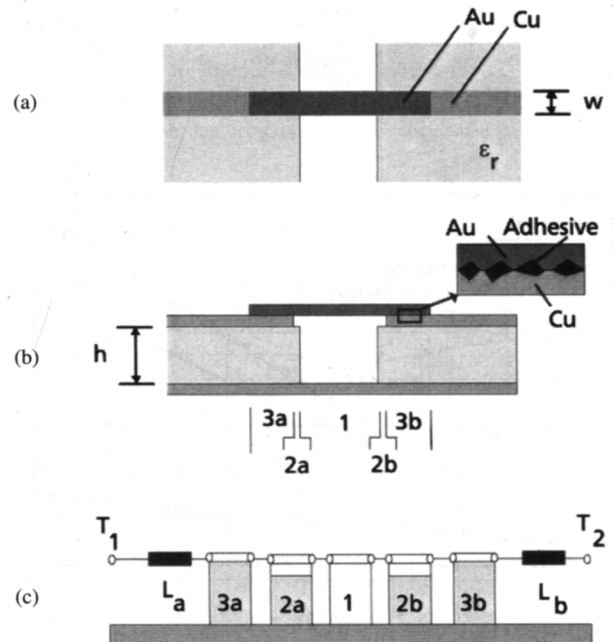


Fig. 1. Derivation of an equivalent circuit for an adhesive ribbon bond connection.

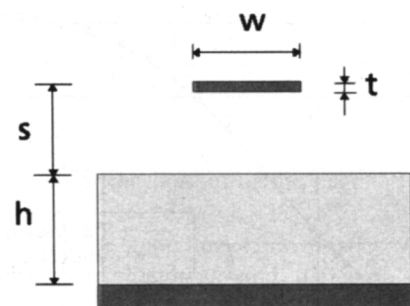


Fig. 2. Cross section of the lines 2a and 2b.

a loop is avoidable. This reduces the parasitic inductance, and the interconnection is use upable to 50 GHz or more. This interconnect technique will be discussed in the following.

The work is organized in two parts. The first part presents a quasistatic approach for the analysis of adhesive bonded ribbon interconnections. The fabrication and the experimental characterization of such a microstrip-to-microstrip interconnect for millimeterwave applications is discussed in the second part.

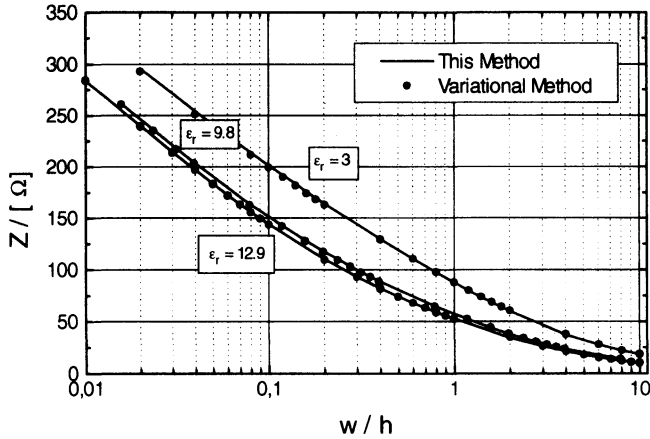


Fig. 3. Calculated Z versus w/h with ϵ_r as parameter ($t = 0 \mu\text{m}$, $s/h = 0.02$).

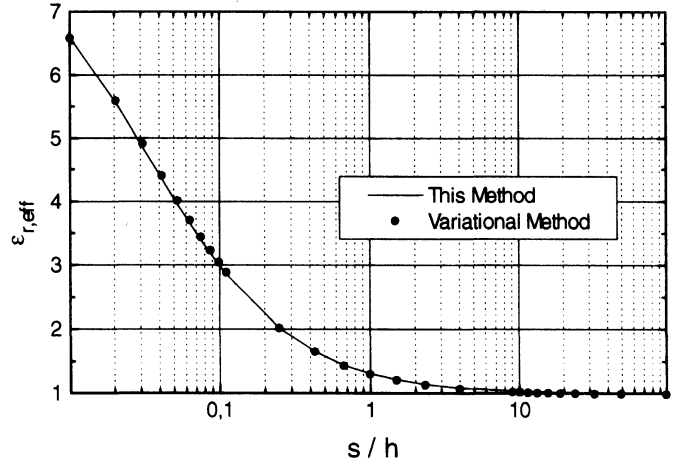


Fig. 6. Calculated $\epsilon_{r,\text{eff}}$ versus the spacing between ribbon and substrate with $\epsilon_r = 12.9$, $t = 0 \mu\text{m}$, and $w/h = 0.7$.

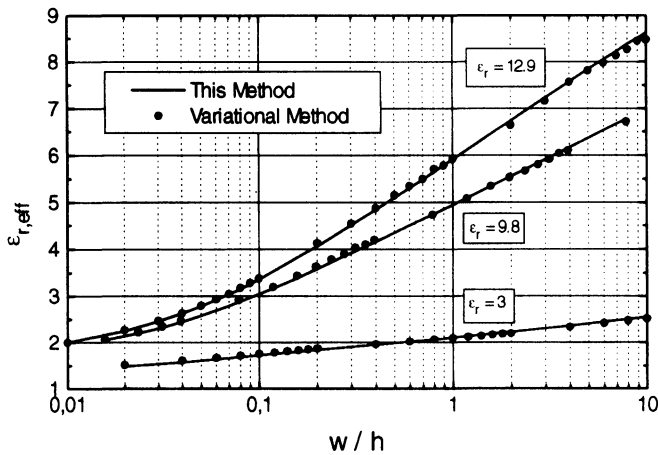


Fig. 4. Calculated $\epsilon_{r,\text{eff}}$ versus w/h with ϵ_r as parameter ($t = 0 \mu\text{m}$, $s/h = 0.02$).

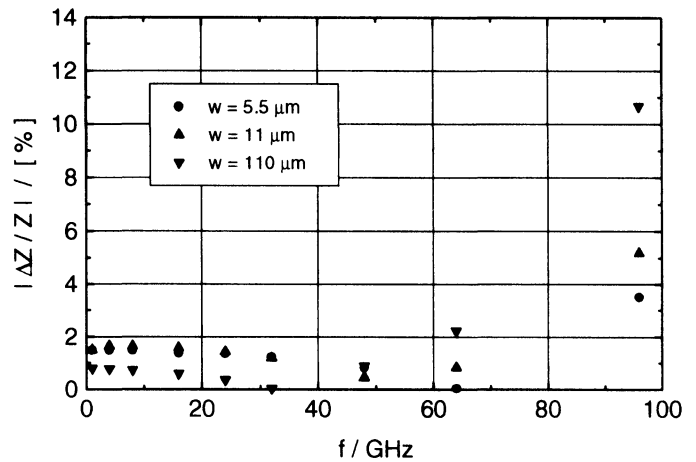


Fig. 7. Dispersion of the characteristic impedance.

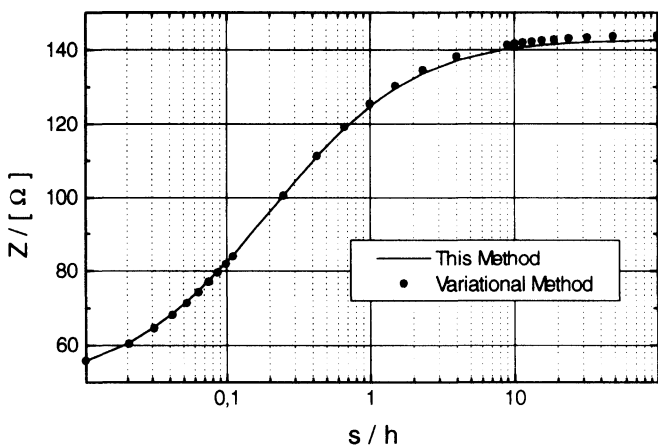


Fig. 5. Calculated Z versus s/h with $\epsilon_r = 12.9$, $t = 0 \mu\text{m}$ and $w/h = 0.7$.

II. SIMULATION

A typical assembly of an interconnection with an adhesive bonded ribbon of two planar circuits having identical height is shown in Fig. 1(a) and (b). An automated diebond process requires a certain mounting gap between the chips. Usually the bond pads end at some distance in the chip edges. Errors in

the placement of the chips during assembly and mechanical tolerances in the chip size cause significant variations of the distance between the bond pads [8]. A thin layer of a two component epoxy is used as adhesive and the electrical conductivity is realized by direct contact of the microstrip conductor and the Au-ribbon. In the following this will be called "narrow gap adhesive joint." The contact resistance at each joint of an adhesive bonded ribbon connect has been measured with the four point probe method. This resistance is relatively small (about $10 \text{ m}\Omega$) and could be neglected during the simulation.

The analysis of a microstrip-to-microstrip interconnect with an adhesive bonded ribbon is a complicated three-dimensional (3-D) field problem because the structure is open and vertical dielectric boundaries are involved. A full-wave method requires a considerable numerical effort, i.e., much memory capacity and CPU time, to compute the performance of this discontinuity. In addition, the input needed to vary the geometric parameters is extensive. The functional dependence of the interconnect properties on geometric parameters is accessible via a quasistatic approach. Here, such a model is developed for the analysis of microstrip adhesive bonded ribbon interconnects.

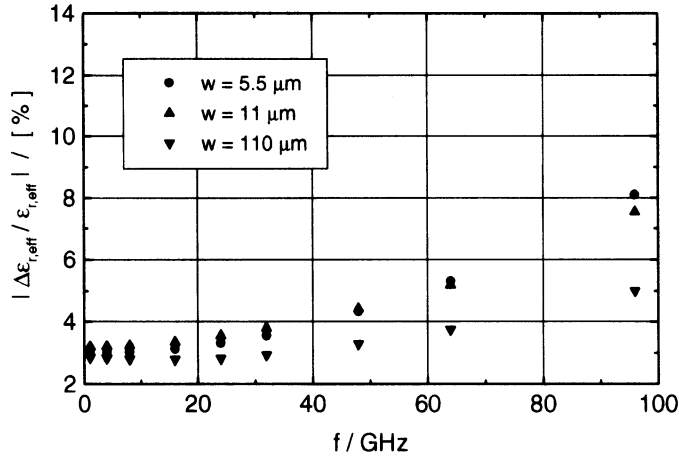


Fig. 8. Dispersion of the effective dielectric constant.

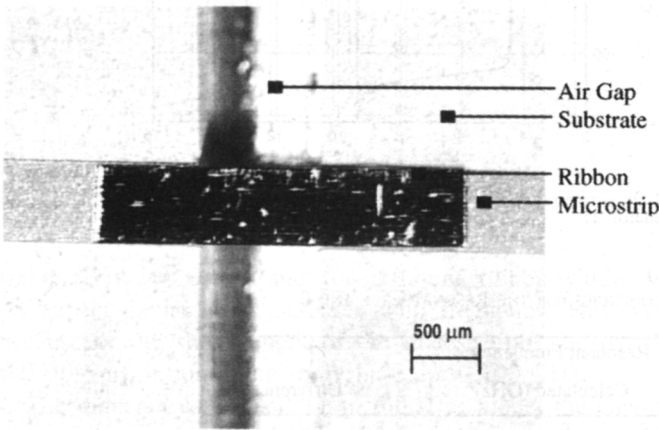


Fig. 9. A typical interconnect with an adhesive bonded ribbon.

The connection is broken down into several sections corresponding to the different parts of the physical arrangement [Fig. 1(b) and (c)]. The quasi TEM lines 3a and 3b model the section of the attachment. The partly dielectric loaded quasi TEM lines 2a and 2b represent the sections from the ends of the bondpads to the edges of the substrates. The homogeneous air line (1), finally, renders the gap between the substrates. The ports of the equivalent circuit are denoted by T1 and T2.

The line sections 1 and 3 are conventional microstrip lines without and with substrate layer, respectively. Their parameters are obtained from standard models (e.g. [11], [12]). For the line sections 2a and 2b corresponding expressions must be developed. The structure to be analyzed consists of a square ribbon over a ground plane covered with a dielectric layer (Fig. 2). A quasistatic model has been used to derive closed form expressions for this transmission line (see Appendix). The approach uses a dividing-the-capacitance approach [13]–[15]. The following expressions for Z and $\epsilon_{r,\text{eff}}$

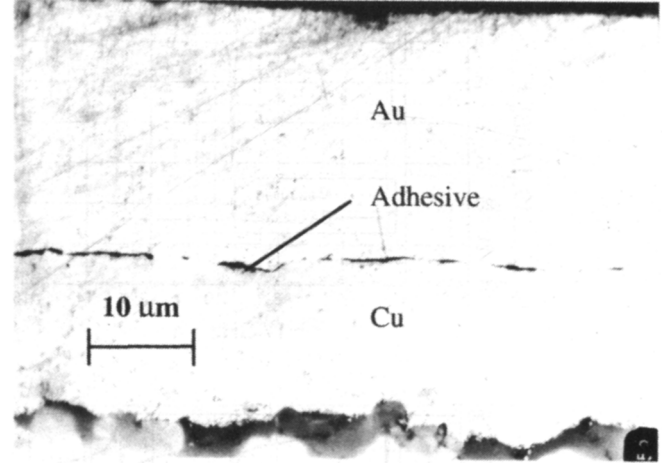


Fig. 10. Cross section of a typical interconnect with adhesive bonded ribbon.

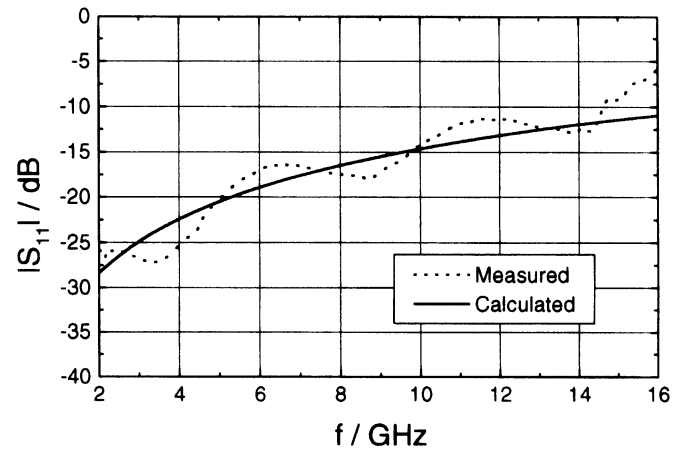


Fig. 11. Comparison of measured and calculated return loss of the interconnection in Fig. 9.

are obtained

$$Z = \sqrt{Z_{\text{stat}2}^2 + \frac{Z_{02} \cdot Z_{\text{stat}1}^2}{Z_{01}} + Z_{01} \cdot Z_{02}} \quad (1)$$

and (2) as shown at the bottom of the page.

Here, $\epsilon_{r,\text{eff},\text{stat}1} = \epsilon_{r,\text{eff},\text{stat}}(w, s, \epsilon_r)$ and $Z_{\text{stat}1} = Z_{\text{stat}}(w, s, \epsilon_r)$ are the static line characteristics of a microstrip with a substrate of height s and dielectric constant ϵ_r ; $\epsilon_{r,\text{eff},\text{stat}2} = \epsilon_{r,\text{eff},\text{stat}}(w, h + s, \epsilon_r)$ and $Z_{\text{stat}2} = Z_{\text{stat}}(w, h + s, \epsilon_r)$ are the same quantities for a substrate of height $h + s$. Further, $Z_{01} = Z_0(w, s, \epsilon_r = 1)$ and $Z_{02} = Z_0(w, h + s, \epsilon_r = 1)$ are the characteristic impedances of microstrip lines without substrate. The expressions for the line characteristics can be found, for example, in [22] and [23].

The results for the line characteristics were verified with a variational method [16], [17]. Calculated results using the derived expressions are compared with the available numerical

$$\epsilon_{r,\text{eff}} = \frac{\epsilon_{r,\text{eff},\text{stat}1} \cdot \epsilon_{r,\text{eff},\text{stat}2} \cdot Z_{02}}{\epsilon_{r,\text{eff},\text{stat}1} \cdot Z_{02} - \epsilon_{r,\text{eff},\text{stat}2} \cdot Z_{01} + \epsilon_{r,\text{eff},\text{stat}1} \cdot \epsilon_{r,\text{eff},\text{stat}2} \cdot Z_{01}} \quad (2)$$

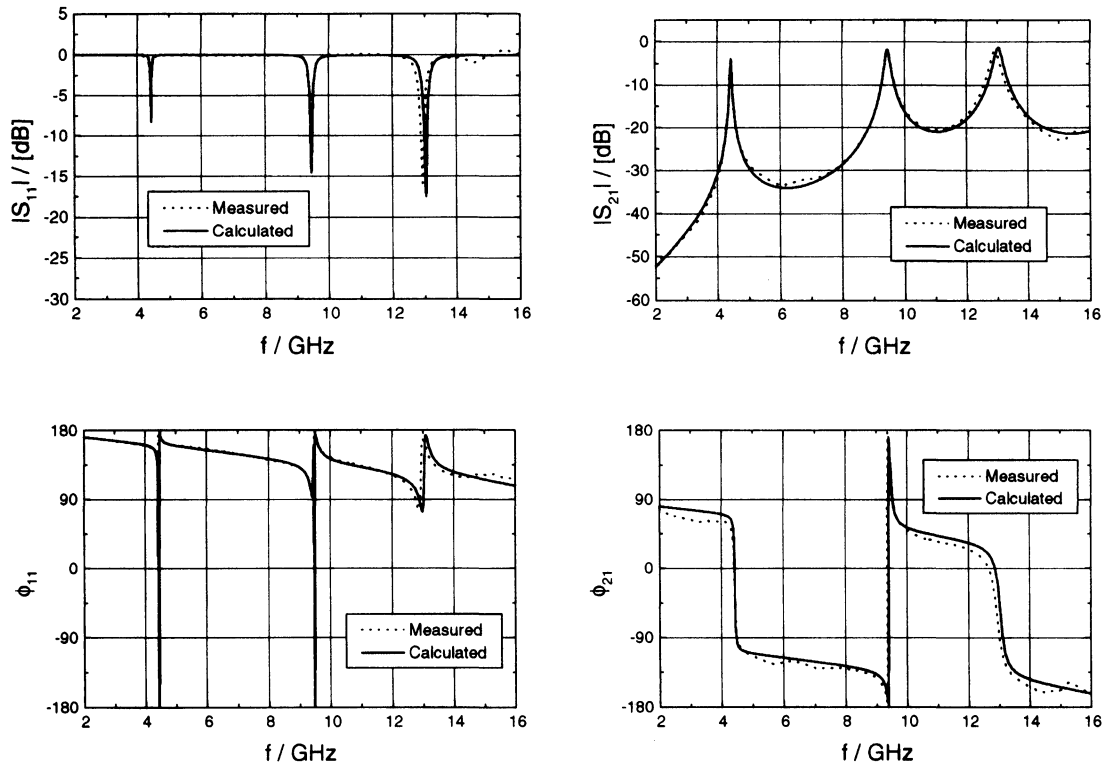

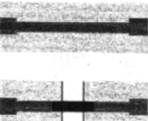
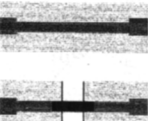
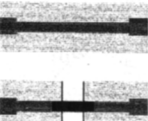


Fig. 12. Comparison of measured and calculated scattering parameters of resonator 1.

TABLE I
EXPERIMENTAL AND CALCULATED RESONANT FREQUENCIES FOR THE RESONATORS 1 AND 2

Microstrip Resonator	Resonant Frequency								
	Measured (GHz)			Calculated (GHz)			% Difference		
	f_{R1}	f_{R2}	f_{R3}	f_{R1}	f_{R2}	f_{R3}	f_{R1}	f_{R2}	f_{R3}
	4,42	8,72	12,94	4,41	8,70	12,90	-0,23	-0,23	-0,31
	f_{R1}	f_{R2}		f_{R1}	f_{R2}		f_{R1}	f_{R2}	
	4,42	9,07	12,85	4,42	9,09	12,94	0,10	0,22	0,70
	f_{R1}	f_{R2}		f_{R1}	f_{R2}		f_{R1}	f_{R2}	
	5,58	11,08		5,61	11,03		0,53	-0,45	
	f_{R1}	f_{R2}		f_{R1}	f_{R2}		f_{R1}	f_{R2}	
	6,49	10,40		6,50	10,37		0,15	-0,29	

results of the variational method in Figs. 3 and 4. This comparison is done for three substrate materials, namely RT-Duroid ($\epsilon_r = 3$), Aluminumoxide ($\epsilon_r = 9.8$) and Gallium Arsenide ($\epsilon_r = 12.9$). The ratio of the air gap height s and the substrate height h is $s/h = 0.02$, w is the ribbon width and t the thickness of the ribbon.

The agreement between the two methods is very close, the relative difference remaining below 1% for the characteristic impedance and 2% for the effective dielectric constant. Figs. 5 and 6 show a comparison between the modeled values and the values obtained by the variational method for the impedance and the effective dielectric constant of a GaAs substrate with $w/h = 0.7$ by varying the ratio s/h , respectively. In this case,

the error is less than 1%, too. It should be remarked, that the error increases for a ratio t/s larger than 1, if the thickness of the ribbon will be taking into consideration with the concept of effective width suggested by Wheeler [22].

The dispersion of the line characteristics can be approximated by replacing the corresponding static quantities in (1) and (2) by frequency dependent expressions [11], [12].

The frequency dependence of the characteristic impedance and of the effective dielectric constant calculated using the derived expressions are compared with the data obtained from a spectral domain moment method approach. The relative differences are shown versus frequencies in Figs. 7 and 8, respectively, for a gallium arsenide substrate, a finite thickness

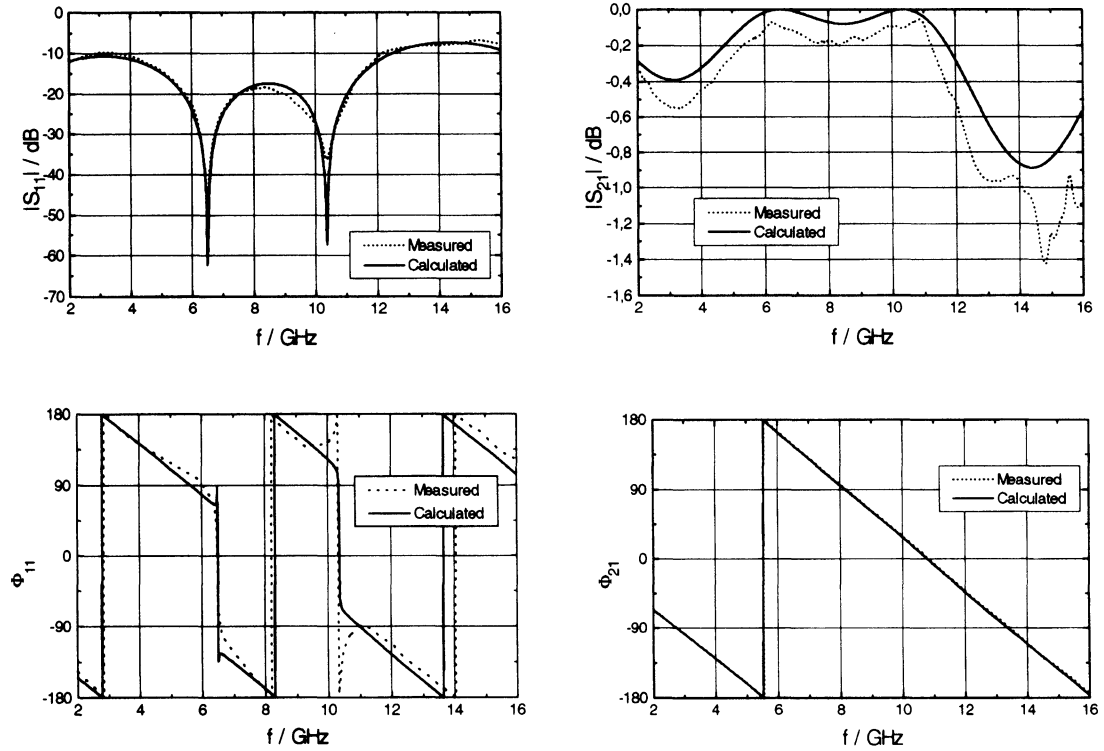


Fig. 13. Comparison of measured and calculated scattering parameters of resonator 2.

ribbon, $s/h = 0,02$ and for different ribbon-widths w . As expected, the error increases with frequency. However, because of the short length of the line sections 2a and 2b (20–30 μm), it contributes only little up to 100 GHz.

The inductances L_a and L_b in Fig. 1(c) model the change in the strip conductor thickness of the microstrip line in the bonding area. They were calculated by means of an equivalent waveguide model [18]–[20]. Here, the change in the strip conductor thickness is taken into account by a step of the strip width for which standard models are available [21].

The transition from line section 1 to line section 2 can be calculated adequately by changing the effective dielectric constant. Results show that this assumption leads to negligible errors.

III. EXPERIMENTAL VERIFICATION

The analytical model was verified at lower frequencies in a scaled experiment, because no mm-wave probing station was available. The microstrip lines were designed with a length of 20 mm on a 635 μm thick substrate. A dielectric constant of 10.8, close to the GaAs value ($\epsilon_r = 12.9$), was chosen. The width of the microstrip conductor was 547 μm (scaling factor 6). The microstrip-line was symmetrically cut into two parts to allow an adjustable air gap. This airgap was then electrically bridged with an Au-ribbon and a two component epoxy adhesive. Fig. 9 shows a typical microstrip-to-microstrip interconnect of two RT-Duroid substrates with an adhesive bonded ribbon. The adhesive is located in the microcavities of the rough surfaces (Fig. 10) thus providing a direct contact of the microstrip conductor with the Au-ribbon. A two component, thermally curing epoxy adhesive was used.

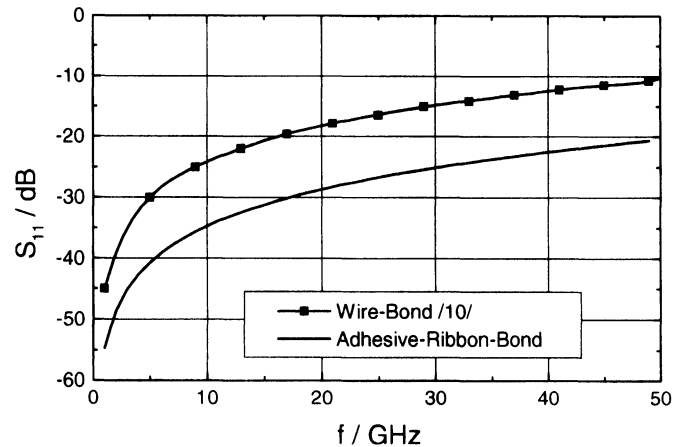


Fig. 14. Simulated reflection coefficient of a wire-bond after [10] and an adhesive bonded ribbon interconnect.

The adhesive was dispensed with an optimized pneumatic dispenser. After the dispensing of the adhesive the Au-ribbon was mounted.

The scattering parameters of this interconnect were measured using a network analyzer (HP8510C). The network analyzer was calibrated inside a test fixture (Wiltron, Universal Test Fixture 3680) using TRL standards. The measured and calculated return loss of a line with one interconnection shows Fig. 11. The measured return loss exhibits mismatch ripples because of the insufficient reproducibility of the contacts between the test fixture and the test device. This makes the direct measurement of the scattering parameters of the interconnect impossible; to increase the sensitivity the discontinuity was tested in two resonator structures. Resonator 1 (length: 12

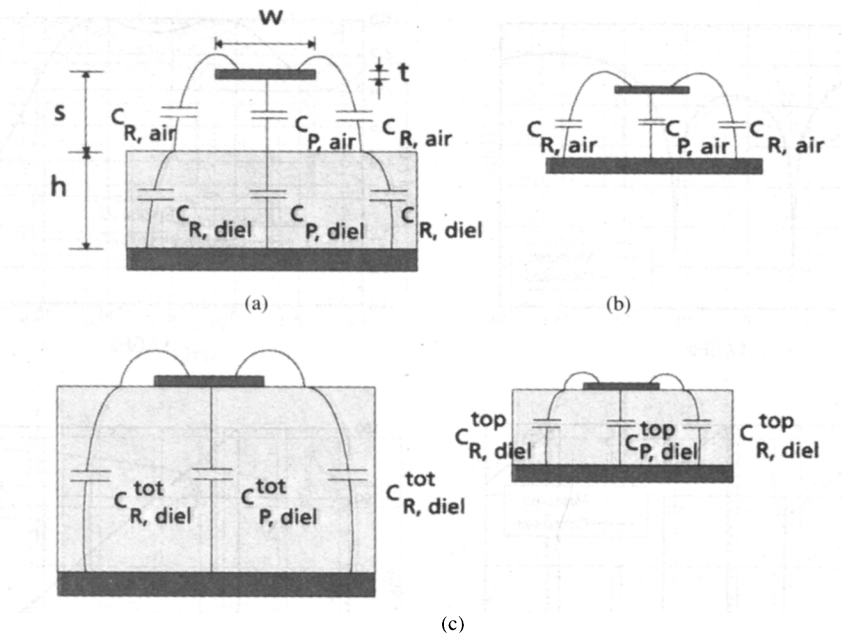


Fig. 15. (a) Cross section of the microstrip like transmission lines 2a and 2b. (b) Determination of C_{air} . (c) Determination of C_{diel} .

mm) is coupled via two gaps while resonator 2 (length: 10 mm) simply exhibits a different line impedance. An airgap cut in the middle of the resonators was then bridged by a ribbon. The exact mechanical dimensions of the interconnect and the resonator were measured optically and taken for the analysis. Figs. 12 and 13 show a comparison of the calculated and measured scattering parameters. The agreement is quite satisfactory. Table I summarizes the experimental and calculated resonant frequencies for resonators 1 and 2 both without airgap and with an adhesive bonded ribbon interconnect. The agreement between measured and calculated values for resonator 1 without airgap is within 0, 3%. With a bridged gap the prediction is within 0, 1% for the first and within 0, 22% for the second resonant frequency. The difference between simulation and experiment increases with frequency, because of the decreasing accuracy of the quasistatic approach and reaches 0, 7% at the third resonance. For resonator 2 the difference remains below 0.5% for the first two resonances. The good agreement between simulation and experiments and the little numerical effort involved justifies the use of the quasistatic model.

IV. APPLICABILITY TO MILLIMETERWAVE ASSEMBLIES

To explore the potential of the adhesive ribbon interconnects bonding technique the quasistatic model was used to predict their performance at mm-wave frequencies, thus allowing a comparison to standard bonding techniques.

Typically, MMIC's and M³IC's are fabricated on GaAs-substrates with heights of 100, 127, and 152 μm . Two identical GaAs-substrates with 50 Ω microstrips are connected. With reference to Fig. 1 the height of the substrate is 100 μm , the length of the airgap 100 μm and the length of section 3a,b 150 μm while the strip-width is 75 μm . The dimension of the ribbon is 75 \times 25 μm . Fig. 14 shows a comparison between a wire-bond interconnection (the wire diameter is 25

μm) and an adhesive bonded ribbon interconnection. The chip interconnect with the adhesive bonded ribbon shows a better electrical behavior in the millimeter wave range than the wire-bond interconnection. The reflection coefficient S_{11} remains below -20 dB up to 50 GHz. This result demonstrates the applicability of this new interconnection technique at micro- and millimeterwave frequencies. Simulations which use wider ribbons show, that operating frequencies of 100 GHz and more are realizable.

V. CONCLUSION

A quasistatic approach for the analysis of microstrip-to-microstrip interconnects with adhesive bonded ribbons has been developed. The analysis of these interconnects shows that it is possible to achieve low insertion loss microstrip interconnects in microwave assemblies. Such interconnects were fabricated and measured. The simulations were shown to be in good agreement with the experimental results thus validating the model. Investigations of scaled structures promise excellent applicability of this interconnection technique in micro- and millimeterwave assemblies.

APPENDIX

In general, the total capacitance of a microstrip line C_{MS} can be broken up into parallel-plate (C_P) and fringing parts (C_R) [15]

$$C_{MS} = C_P + 2 \cdot C_R. \quad (3)$$

The structure to be analyzed consists of a square ribbon over a ground plane covered with a dielectric layer [Fig. 15(a)]. The capacitances of this structure can be split into terms for the air and the dielectric capacitances connected in series.

In case of a high dielectric constant layer, the electric field lines are approximately normal to the air-substrate boundary,

which is then almost an equipotential line. Calculated results show that this assumption leads to only negligible errors. Then the capacitance is given by

$$C_S = \frac{C_{\text{air}} \cdot C_{\text{diel}}}{C_{\text{air}} + C_{\text{diel}}} \quad (4)$$

with

$$\begin{aligned} C_{\text{air}} &= C_{P,\text{air}} + 2 \cdot C_{R,\text{air}} \\ C_{\text{diel}} &= C_{P,\text{diel}} + 2 \cdot C_{R,\text{diel}} \end{aligned}$$

With the above assumptions the structure can be decomposed into conventional microstrip lines as shown in Fig. 15(b) and (c). Assuming further that $C_{\text{diel}}^{\text{tot}}$ is the series connection of $C_{\text{diel}}^{\text{tot}}$ and C_{diel} the capacitances C_{air} and C_{diel} can be obtained from

$$C_{\text{air}} = C_o^{\text{air}} = \frac{1}{c_o \cdot Z_0(w, s, \varepsilon_r = 1)} \quad (5)$$

and

$$C_{\text{diel}} = \frac{C_{\text{diel}}^{\text{tot}} \cdot C_{\text{diel}}^{\text{top}}}{C_{\text{diel}}^{\text{top}} - C_{\text{diel}}^{\text{tot}}} \quad (6)$$

with

$$C_{\text{diel}}^{\text{top}} = \frac{Z_o(w, s, \varepsilon_r = 1)}{c_o \cdot Z_L^2(w, s, \varepsilon_r)}$$

and

$$C_{\text{diel}}^{\text{tot}} = \frac{Z_o(w, h + s, \varepsilon_r = 1)}{c_o \cdot Z_L^2(w, h + s, \varepsilon_r)}$$

The expressions for $Z_o(\varepsilon_r = 1)$ and Z_L can be found, for example, in [11], [22], [23].

The characteristic impedance and the effective dielectric constant of the microstrip-like transmission line with an airgap between the dielectric substrate and the ribbon are obtained from

$$Z = \frac{1}{c_o \cdot \sqrt{C_S \cdot C_S^{\text{air}}}} \quad (7)$$

and

$$\varepsilon_{r,\text{eff}} = \frac{C_S}{C_S^{\text{air}}} \quad (8)$$

ACKNOWLEDGMENT

The authors would like to thank G. Oberschmidt for the results of the spectral domain moment method approach.

REFERENCES

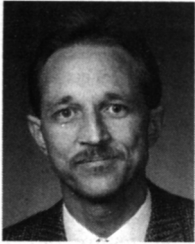
- [1] U. Goebel, "DC to 100 GHz chip-to-chip interconnects with reduced tolerance sensitivity by adaptive wirebonding," in *Proc. IEEE 5th Topical Elect. Performance Electron. Packag.*, Monterey, CA, 1994, pp. 182–185.
- [2] R. Bitz, "Wire-mesh verbindungstechnik für HF-anwendungen," Published by VDI/VDE Technologiezentrum Informationstechnik GmbH, in *Proc. AVT-KEO Abschlußpräsentation*, Berlin, Germany, Nov. 1995.
- [3] H. Richter, "Flip chip attach of GaAs-devices and application to millimeter wave transmission systems," in *Proc. 4th Int. Conf. Micro Electro. Opto. Mech. Syst. Comp.*, Berlin, Germany, Oct. 19–21, 1994, pp. 535–543.

- [4] T. Ohsaki, "Electronic packaging in the 1990's—A perspective from asia," *IEEE Trans. Comp., Hybrids Manufact. Technol.*, vol. 14, pp. 254–261, June 1991.
- [5] G. Strauß and W. Menzel, "Millimeter-wave MMIC interconnects using electromagnetic field coupling," in *Proc. 3rd Topical Meeting Elect. Performance Electron. Packag.*, Monterey, CA, 1994, pp. 142–144.
- [6] J. J. Burke and R. W. Jackson, "Surface-to-surface transition via electromagnetic coupling of microstrip and coplanar waveguide," *IEEE MTT*, vol. 37, pp. 519–525, Mar. 1989.
- [7] F. Alimenti, U. Goebel, and R. Sorrentino, "Quasi static analysis of microstrip bondwire interconnects," *IEEE Trans. Microwave Theory Tech.*, pp. 679–682, 1995.
- [8] U. Goebel, M. Boheim, and F. Farasat, "Adaptive wire bonding for millimeterwave frequencies," *VTE*, no. 4, Dec. 1994.
- [9] M. Boheim, R. Dolp, U. Goebel, and W. Hager, "Innovative packaging in injection moulding technology for mm-wave circuits," in *Proc. 4th Int. Conf. Micro Electro. Opto. Mech. Syst. Comp.*, Berlin, Germany, Oct. 1994, pp. 623–631.
- [10] U. Goebel, "Effiziente elektrische modellierung adaptiver drahtbondverbindungen im millimeterwellenbereich," published by VDI/VDE Technologiezentrum Informationstechnik GmbH, in *Proc. AVT-KEO Abschlußpräsentation*, Berlin, Germany, Nov. 1995.
- [11] R. H. Jansen and M. Kirschning, "Arguments and an accurate mathematical model for the power-current formulation of microstrip characteristic impedance," *Arch. Elektronik u. Übertragungstechn.* 37, 1983.
- [12] M. Kirschning and R. H. Jansen, "Accurate model for effective dielectric constant of microstrip with validity up to millimeter-wave frequencies," *Electron. Lett.*, vol. 18, no. 6, pp. 272–273, 1982.
- [13] S. S. Bedair, "Predict enclosure effects on shielded microstrip," *Microwaves RF*, pp. 97–100, 1985.
- [14] ———, "Closed form expressions for the static capacitances of some microstrip disk resonators," *Arch. Elektron. Uebertragungstechn.*, vol. 39, pp. 269–272, 1985.
- [15] ———, "Closed form expressions for the computer-aided design of suspended microstrip circuits for millimeter wave applications," *IEE Proc*, vol. 134, pp. 386–388, Aug. 1987.
- [16] E. Yamashita and R. Mittra, "Variational method for the analysis of microstrip lines," *IEEE Trans. Microwave Theory Tech.*, vol. MTT-16, pp. 251–256, Apr. 1968.
- [17] E. Yamashita, "Variational method for the analysis of microstrip-like transmission lines," *IEEE Trans. Microwave Theory Tech.*, vol. MTT-16, pp. 529–535, Aug. 1968.
- [18] T. S. Chu, T. Itoh, and Y. C. Shih, "Comparative study of mode-matching formulations for microstrip discontinuity problems," *IEEE Trans. Microwave Theory Tech.*, vol. MTT-30, pp. 1018–1023, Oct. 1985.
- [19] W. Menzel and I. Wolff, "A method for calculating the frequency-dependent properties of microstrip discontinuities," *IEEE Trans. Microwave Theory Tech.*, vol. MTT-25, pp. 1018–1023, Feb. 1977.
- [20] G. Komp, "Frequency-dependent behavior of microstrip offset junctions," *Electron. Lett.*, vol. 11, no. 22, pp. 537–538, Oct. 1975.
- [21] J. Schwinger and D. S. Saxon, "Discontinuities in waveguides." New York: Gordon and Breach, 1968.
- [22] H. A. Wheeler, "Transmission-line properties of a strip on a dielectric sheet on a plane," *IEEE Trans. Microwave Theory Tech.*, vol. MTT-25, pp. 631–647, Aug. 1977.
- [23] ———, "Transmission-line properties of parallel strips separated by a dielectric sheet," *IEEE Trans. Microwave Theory Tech.*, vol. MTT-13, pp. 172–185, 1965.



Wolfgang Pohlmann received the diploma in electrical engineering from the Technical University of Braunschweig, Germany, in 1994 and is currently pursuing the Ph.D. degree.

He works on microjoining technology at the Fraunhofer Institute for Applied Materials Research, Bremen, German. His current research involves new chip-to-chip interconnect techniques for micro and millimeterwave applications.



Arne F. Jacob (S'79–M'81) was born in Braunschweig, Germany, in 1954. He received the Dipl.-Ing. and Dr.-Ing. degrees from the Technische Universität, Braunschweig, Germany, in 1979 and 1986, respectively.

From 1986 to 1988, he was a Fellow at CERN, The European Laborator for Particle Physics, Geneva, Switzerland. From 1988 to 1990, he was with the Accelerator and Fusion Research Division, Lawrence Berkeley Laboratory, University of California, Berkeley, CA. Since then he has been a

Professor at the Institut für Hochfrequenztechnik, Technische Universität, Braunschweig. His current research interests include the design and application of planar circuits at microwave and millimeter frequencies, and the characterization of complex materials.



Helmut Schäfer received the diploma and Ph.D. degrees in material science from the Technical University of Darmstadt, Darmstadt, Germany.

In 1984, he joined the Fraunhofer Institute for Applied Materials Research (IFAM), Bremen, Germany. He is with the Division of "Adhesive Bonding Technology and Polymers," and currently leads the R&D activities on micro-joining technology.